Critical Elements in Magnet Cove Carbonatites

Ross Clark

Advisors: Dr. Philip Piccoli and Dr. Richard Ash

Geol 394

Scientific Abstract

Critical elements (or minerals) are natural resources that are crucial for modern technologies that have a significant risk for supply chain disruption (DOE, 2024). With the current state of world politics, the US government is looking for domestic production and refinement of these resources. Notable examples of critical elements include the use of indium for touchscreens and niobium as an anticorrosive and in superconductors. While the exact list of critical elements varies between government agencies due to differing priorities (Rowan, 2024), though some such as rare earth elements (REEs), remain consistent throughout. All REEs have uses in modern technologies, some examples include neodymium, which is used to create permanent magnets, and gadolinium, which is used as contrast for magnetic resonance imaging (MRI). Carbonatites are rare igneous rocks, with approximately 550 total locations worldwide (Woolley and Kjarsgaard, 2008), that contain greater than 50% carbonates. REEs and other critical elements are often enriched in carbonatites. Nine percent of all known carbonatite localities have or were historically mined (Simandl and Paradis, 2018). While REEs are common in crustal rocks significant concentrations are required to be considered a mineral resource. This study is looking at the critical element enrichment of the carbonatite and related alkali rocks of Magnet Cove, Arkansas and determining the distribution of critical minerals and possible mode of formation. The Magnet Cove Complex is within the Ouachita Mountains in central Arkansas and is about 12 km 2 of surface exposure. There are 5 primary rock types that are seen at this location, jacupirangite, nepheline syenite, trachyte/phonolite, ijolite, and carbonatite (Howard and Chandler, 2007). The carbonatite is less than 2% of the total surface area. The carbonatite is significantly more concentrated than the silicate rocks in REE but over an order of magnitude less concentrated than that of productive carbonatite mines. We see that the whole rock concentrations match the trends that are seen in other carbonatites but in lower concentrations. This likely indicates a depleted source.

Plain text abstract

Critical elements (or minerals) are natural resources that are crucial for modern technologies that have a significant risk for supply chain disruption. With the current state of world politics, the US government is looking for domestic production and refinement of these resources. Notable examples of critical elements include the use of indium for touchscreens and niobium as an anticorrosive and in superconductors. While the exact list of critical elements varies between government agencies due to differing priorities, though some such as rare earth elements (REEs), remain consistent throughout. All REEs have uses in modern technologies, some examples include neodymium, which is used to create permanent magnets, and gadolinium, which is used as contrast for magnetic resonance imaging (MRI). Carbonatites are rare igneous rocks that contain greater than 50% carbonates. They are often the highest producing sources for REEs and other critical minerals. Nine percent of all known carbonatite localities have or were historically mined (Simandl and Paradis, 2018). While REEs are common in crustal rocks significant concentrations are required to be considered a mineral resource. This study is looking at the critical element enrichment of the carbonatite and related alkali rocks of Magnet Cove, Arkansas and determining the distribution of critical minerals and possible mode of formation. The Magnet Cove Complex is within the Ouachita Mountains in central Arkansas and is about 12 km 2 of surface exposure. There are 5 primary rock types that are seen at this location, jacupirangite, nepheline syenite, trachyte/phonolite, ijolite, and carbonatite (Howard and Chandler, 2007). The carbonatite is less than

2% of the total surface area. The carbonatite is significantly more concentrated than the silicate rocks in REE but over an order of magnitude less concentrated than that of productive carbonatite mines.

1. INTRODUCTION AND BACKGROUND

1.a. What are Critical Minerals?

Critical minerals are defined as “nonfuel minerals that is essential for use and faces considerable supply chain vulnerabilities” (Rowan, 2022). Lists are extensive and encompass 50+ elements and minerals. While they are called “critical minerals” most are listed in the elemental state. The exact list varies from agency to agency, but many elements are shared in each list. Such as the rare earth elements (REEs) that are predominately found in carbonatites and are used for batteries and in alloys. The current list of critical minerals was recently changed so that copper, helium, potassium, lead, silver and uranium are no longer considered critical. Reasons why elements are taken off the list vary, such as copper and helium which were taken off due to the lack of supply chain disruption (Rowan, 2024). Or uranium which is now defined as a fuel element and therefore does not meet the current definition set forth by the DOE and USGS.

These are especially important in the current political climate with constant uncertainty of sourcing

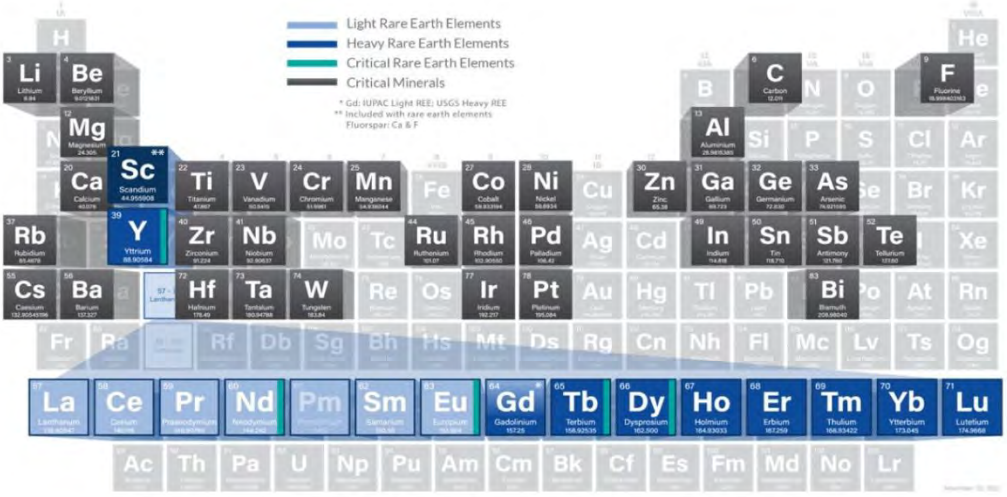

Figure 1: A chart highlighting all the current critical elements (plus calcium and promethium) as well as breaking down the REE into LREE and HREE; (DOE, 2024)

critical minerals. In 2024, 12 critical minerals the US was entirely reliant on imports as well as 28 that were more than 50% imported. Growing political tension with especially China has made obtaining certain critical minerals such as REEs difficult. However, the US government is investing heavily in mines and refineries and have promised to pay twice market rates for REEs. This incentivizes the exploration of new potential sources for these resources including carbonatites such as is seen at Magnet Cove, Arkansas.

1.b. What are Carbonatites?

Carbonatites are defined as igneous rocks that are >50% carbonates. These are rare with about 550 total known locations around the world (Wooley, 2008) (figure 2). Most of these are very small. The 3 major types of carbonatites, calcite, dolomite and ankerite, are defined by the primary carbonate mineral that makes them up (Winter, 2010). There are other types as well, most notably the alkaline natrocarbonatites found only in East Africa at the Oldoinyo Lengai volcano (only known active carbonatite volcano). Like this volcano carbonatites have generally been associated with continental rifts (Simdahl and Paradis, 2018). Carbonatites form from upper mantle melting and are thought to form either from fractional crystallization or liquid immiscibility (Yaxley et al., 2022). Due to differentiation during formation carbonatites are known for their enrichment in REEs and niobium (Wang et al., 2020).

Less than one percent of prospected exploration sites are viable for mining, however, 9% of all known carbonatite intrusions are or have been historically mined for critical minerals (Mitchell, 2005). Not only are carbonatites more frequently viable for mining more than 90% of REEs are mined from carbonatite mines, the two largest being Mountain Pass, CA and Bayan Obo, China.

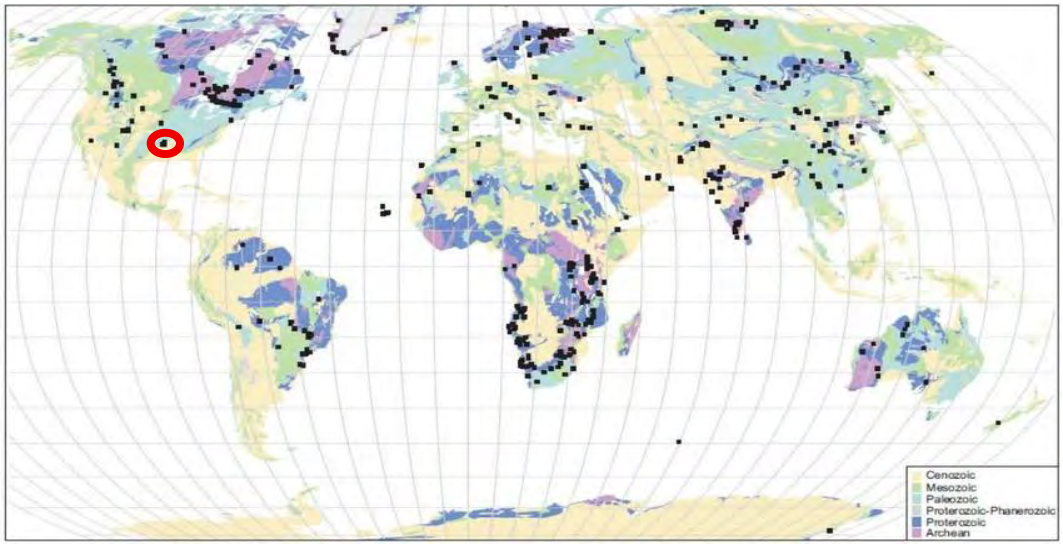

Figure 2: World carbonatite distribution as presented (Wooley and Kjarsgaard, 2008), with magnet cove location indicated

1.c.

Magnet Cove

The Magnet Cove Igneous Complex (MCIC) is a series of small igneous intrusions near Hot Springs, Arkansas. The MCIC has an exposed surface area of approximately 12 km^2 and the carbonatite intrusion is about 2% of the total surface area (Amaral, 2024).

Located within the Ouachita Mountains in central Arkansas, the MCIC is comprised of five major rock types (figure 3). These rock types are jacupirangite, nepheline syenite, trachyte/phonolite, ijolite, and carbonatite.

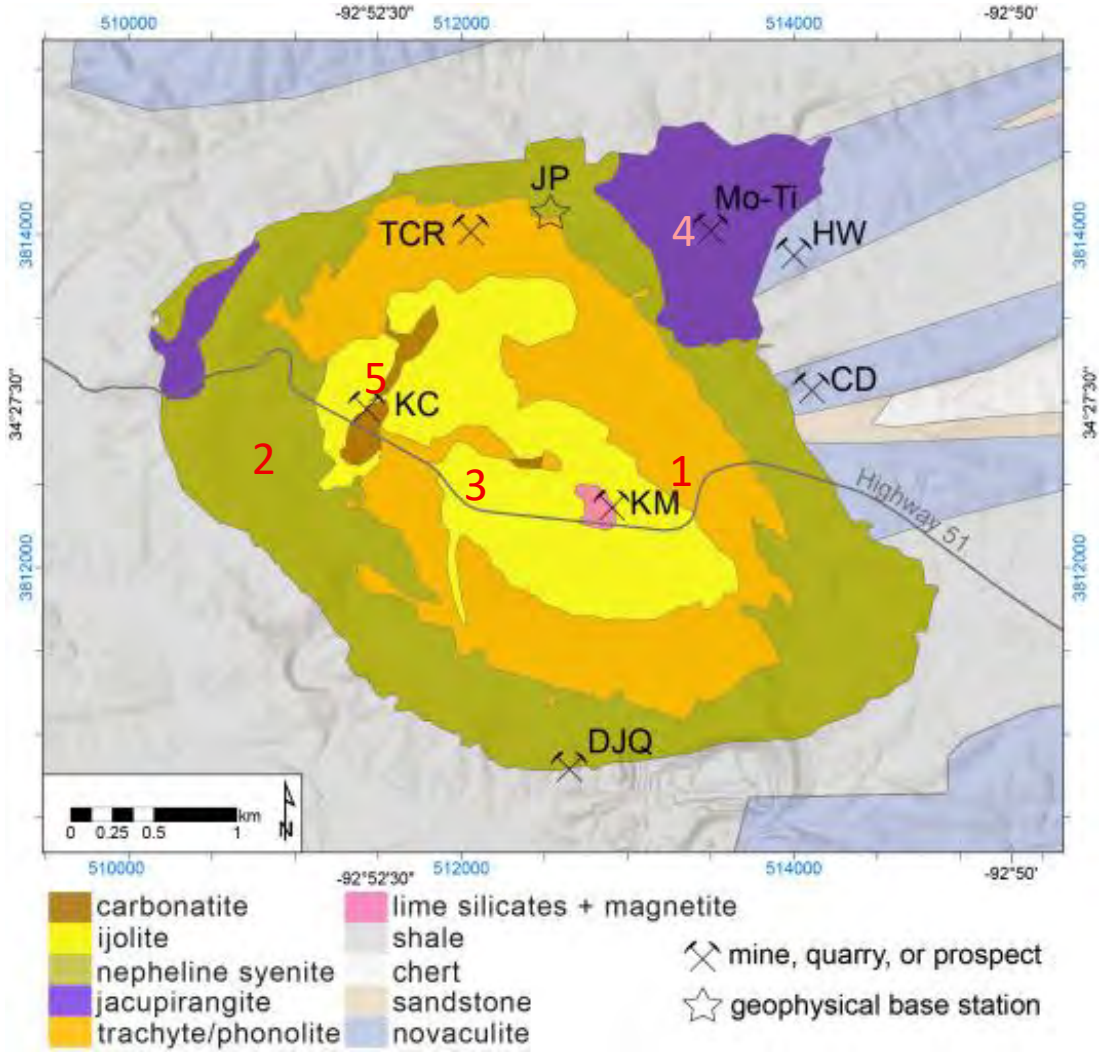

Figure 3: a breakdown of the location of each rock type in the Magnet Cove Igneous Complex (Amaral, 2024) with sample collection locations marked

- Jacupirangite is primarily greater then 50% titanium rich pyroxene.
- Nepheline syenite is a foid bearing potassium feldspar rich plutonic rock.
- Trachyte/phonolite is similar composition to the syenite but is a volcanic rock.
- Ijolite is primarily comprised of augite and nepheline.
- Carbonatite is greater than 50% carbonate

OBJECTIVES OF RESEARCH AND BROADER IMPLICATIONS

With the need for REEs and other critical minerals growing more data is needed how they are distributed in the rocks they are found in relatively high concentrations. Most of the research in this field is focused on how the deposits with exceptionally high concentrations are formed, however, in the preliminary work for this site we found that the concentrations are an order of magnitude lower than

these super enriched regions. But it is also important that we know why these systems fail to become economic.

- Null hypothesis: REE concentrations and distribution will be similar to productive carbonatite locations
- Alternative: REE concentrations will be lower and distribution in minerals will be different than productive carbonatite locations

The alternative hypothesis has a couple of different interpretations as to why this might have occurred. The first interpretation is that the original source of the rock was depleted in REEs. This can be seen in the whole rock data when comparing to other carbonatite sites. Where the carbonatite rocks and the silicate rocks will have similar comparative trends but be significantly lower in concentration. The other interpretation is that there are similar total amounts of total REEs but, they spread through both the carbonatite and silicate rocks. This would be due to incomplete fractionation and has been attributed to lower temperatures during formation (Anenburg et al., 2021).

2. EXPERIMENT DESIGN

2.a. Samples

The rock samples for this project were collected by Mike Howard, a 30-year member of the Arkansas geological survey. As an expert on rocks of Magnet Cove he felt that these samples were representative of the area. From the five rock samples, thin sections were analyzed to determine the individual phases present. The location of collection of each samples collection is in table 1.

Rock Type	Sample	Location
Trachyte-Phonolite	MCIC-1	34.45376, -92.85434
Garnet pseudoleucite nepheline syenite	MCIC-2	34.45530, -92.88400
Biotite Ijolite	MCIC-3	34.45248, -92.86485
Jacupirangite	MCIC-4	34.46941, -92.84909
Carbonatite	MCIC-5a	34.45753, -92.87541

Table 1: Reported coordinates of collected samples for each rock type matched with the sample number

2.b. Petrography

Each of the five thin sections were analyzed under a petrographic microscope to determine each phase that was present. This was then compared to Erikson and Blade (1963) (breakdown in table 2)to confirm the phase was reported in previously performed chemistry. Each identified phase is used for future target of later EPMA analysis. The phases were identified using properties such as color, habit, opacity, and birefringence. Each of the thin sections had a suite of minerals.

	Syenite	Jacupirangite	Ijolite	Phonolite	Carbonatite
Orthoclase	30	0	0	37	0
Nephaline	40	0	27	21	0
Diopside	17	78	40	21	0
Garnet	5	1	4	0	2.5
Apatite	4	5	3	1	0
Biotite	0	1	14	0	25
Magnetite	0	4	0	0	2
Pyrite/pyrrhotite	1	4	6	6	0
Calcite	0	4	6	0	66
Perovskite	0	3	0	0	1
Olivine	0	0	0	0	2.5
Hornblende	0	0	0	5	0
Cancirite	0	0	0	6	0
total	97	100	100	97	99

Table 2: breakdown of the reported mineralogy of each rock type (Erikson and Blade 1963). Numbers averaged from the different samples in the report

In the carbonatite six major phases were identified as being apatite, calcite, 2 separate opaque phases (later identified as an iron oxide phase and perovskite), garnet (identified as kimzeyite), and an olivine (identified as monticellite). In Jacupirangite six major phases were identified as diopside, biotite, titanite, perovskite, and apatite. In the ijolite six phases were identified as nepheline, diopside, biotite, apatite, calcite, and perovskite. In Erikson and Blade perovskite was not reported but there was a small crystal seen in the thin section. It will not contribute much to the budget due to the small contribution to the percentage of the rock. However, I wanted to include it as a comparison of phases between rocks. In the phonolite apatite, diopside, nepheline, and cancrinite were identified. In syenite apatite, nepheline, and leucite. In both samples there is a significant amount of ground mass and are significantly altered. The largest portion of these rocks were reported to be orthoclase; however, it was not seen in this rock sample. This is mostly likely in the mixed phase altered ground mass.

2.c. Electron Probe Microanalysis (EPMA)

The JEOL JXA 8900R Electron Probe Microanalyzer was used at the AIMLab at the University of Maryland. The polished thin section was coated with 200-300 Å of carbon to eliminate the charging of the sample. A 1-50 µm beam was used (depending on mineral crystal size) with 10-120 second count times. The machine used a 15 kV accelerating current and 5-20 nA cup current. Raw counts were corrected using a ZAF algorithm.

Analysis of each potential phase analysis was performed using energy dispersive spectroscopy (EDS). The microanalyzer analysis was done on each of the identified minerals. The major element composition of each phase was determined. This needs to be done to determine the minor elemental concentrations when using the LA-ICP-MS as internal standards.

2.d. Laser Ablation Inductively Coupled Plasma Mass Spectrometry (LA-ICP-MS)

LA-ICP-MS analyses were performed to obtain minor and trace element concentrations in each mineral phase at ppm to ppb concentrations. Due to the data from this analysis being relative, the use of internal standards of a major element composition is needed to determine the minor element compositions. The three internal standards that were used were calcium, silica and iron (depending on each which element was dominant in each mineral that was analyzed). Apatite and calcite used

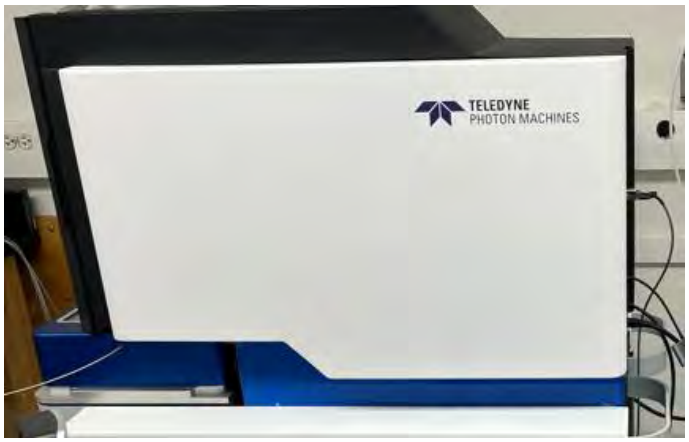

Figure 4: Teledyne Laser used at Carnegie Lab

Analyses of the carbonatite were performed at Carnegie Science, using a teledyne laser (figure 4) in conjunction with an i-CAPQ ICP-MS for this analysis. The elements that were analyzed for were the following: ^{7}Li, ^{23}Na, ^{25}Mg, ^{26}Mg, ^{27}Al, ^{29}Si, ^{30}Si, ^{31}P, ^{43}Ca, ^{45}Sc, ^{47}Ti, ^{49}Ti, ^{51}V, ^{55}Mn, ^{57}Fe, ^{59}Co, ^{60}Ni, ^{61}Ni, ^{63}Cu, ^{64}Zn, ^{66}Zn, ^{86}Sr, ^{88}Sr, ^{89}Y, ^{90}Zr, ^{91}Zr, ^{93}Nb, ^{97}Mo, ^{98}Mo, ^{133}Cs, ^{137}Ba, ^{138}Ba, ^{139}La, ^{140}Ce, ^{141}Pr, ^{142}Nd, ^{144}Nd, ^{146}Nd, ^{147}Sm, ^{151}Eu, ^{152}Sm, ^{153}Eu, ^{154}Sm, ^{155}Gd, ^{157}Gd, ^{159}Tb, ^{161}Dy, ^{163}Dy, ^{165}Ho, ^{166}Er, ^{169}Tm, ^{172}Yb, ^{175}Lu, ^{178}Hf, ^{181}Ta, ^{182}W, ^{232}Th, and ^{238}U. The analysis of the other 4 rock types were analyzed using the Thermofinnigan element 2 at the University of Maryland.

There is significant overlap reading in some of the REE isotopes. To minimize this issue one isotope was selected for analysis for each element. The isotopes used for REE interpretation are: ^{139}La, ^{140}Ce, ^{141}Pr, ^{146}Nd, ^{154}Sm, ^{153}Eu, ^{157}Gd, ^{159}Tb, ^{163}Dy, ^{165}Ho, ^{166}Er, ^{169}Tm, ^{172}Yb, and ^{175}Lu

The data were reduced using the certified sample NIST610 and BHVO-2G as standards. All the measurements of each element were averaged and then divided by the accepted concentrations. This generates a count to concentration conversion factor. Then each concentration is divided by this conversion factor. Then the internal standard for each phase is applied.

3. LIMITATIONS

This approach to analysis is best for comparison of concentrations between different minerals in a rock and concentration of the same mineral in different rocks. This allows for a useful comparison between different rock types using their similarities to normalize the data. However, there are significant limitations with this approach. It is less useful in the whole rock comparison. There are faster and more accurate ways in determining the whole rock composition than the method that is used here. These methods will not show correlation between concentrations and minerals present but has fewer pitfalls in the whole rock analysis. This issue is most seen in the syenite and the phonolite samples. In Erikson and Blade (1963) these rocks are approximately a third orthoclase, but when petrology was conducted there wasn't any orthoclase that was seen. As was previously stated this is likely in the matrix in a mixed phase. Since this analysis is comparing like minerals mixed and altered phases were avoided. This is intentional because determining the exact mineral composition of these mixes would be extremely

difficult and likely not result in any direct comparison. In the future it would probably be a combination of a more destructive analysis that allows for the mixed phases to be incorporated in the final whole rock analysis and the one that was done here. This would also minimize the risk of skewed results in specific crystals of the analyzed minerals being outliers and skewing the results. To compare to other sites this is the primary mode of analysis for determining the content of ore rock. To compare to these other analyses estimating to whole rock will be necessary.

4. RESULTS

4.a Carbonatite

Apatite takes up more than half of the REE budget. Though it takes up a considerable amount more of the LREEs than the HREE. The budget has 79% La and generally trends downwards as the REE become heavier with 66% Lu. Perovskite despite only being approximately a percent of the rocks total makeup has 17-18% of the LREE budget of the rock but this percent drops off the heavier the element is with only about 2% of the total Lu in the rock. Kimzeyite starts with less than a percent of the REE budget of La but the Budget generally trends upward the heavier the element and has a total of 24% Lu. Monticellite follows the same trends as the kimzeyite and has about 5% of the Lu of the rock. Neither calcite or the iron oxide phase have a significant percentage of the REE budget for any element.

4.b Jacupirangite

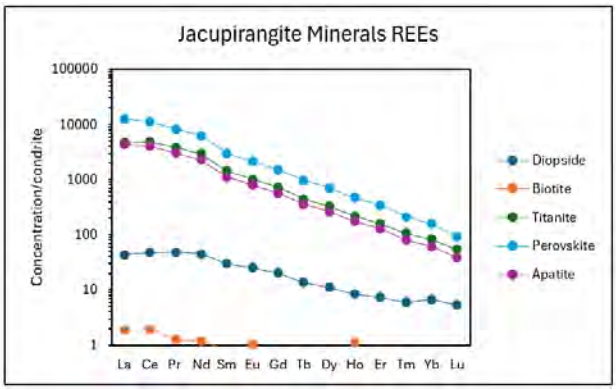

Figure 5: Breakdown of the chondrite normalized (McDonough and Sun 1995) for each mineral analyzed the in jacupirangite sample

The largest portion of the REE budget is stored in the perovskite. The concentration of the REE in the perovskite is about an order of magnitude higher than what is seen in either the apatite or the titanite. Approximately 50% of the LREE budget and 30% of the HREE is in the perovskite though it is only 3% of the total rock. Apatite is 30% of the LREEs and 20% of the HREEs. While the diopside only has 5% of the LREEs it is 45% of the rocks HREE budget. This is due to the rock being majority diopside. As seen in the carbonatite, magnetite and carbonates do not have high concentrations of trace elements and analyses were not included in this or later rock types.

4.c Syenite

In no analyzed phase is there a significant concentration of REEs seen. Though there are a few issues with some of the data. The most glaring as stated before is the missing orthoclase mineral that is most likely in altered mixed phase. Much of the budget of the REEs of this rock are in the apatite, however, even this is between 100-200 normalized values. This is an entire order of magnitude lower than any other apatite seen in the entire complex.

4.d Phonolite

The phonolite Data like the syenite data has some issues. However, the data obtained is still useful for comparison. But of the analyzed minerals apatite is the most concentrated in the Apatite with the Diopside being the dominant host of the HREEs. While the cancrinite follows the same pattern of concentration (though slightly increased) it is significantly less abundant in the rock than the dioside.

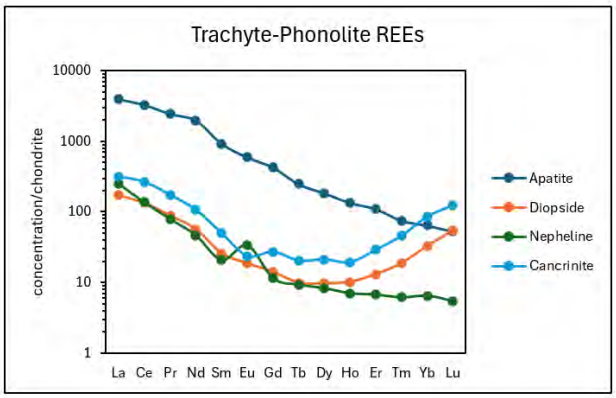

Figure 6: Breakdown of the chondrite normalized (McDonough and Sun 1995) for each mineral analyzed the from phonolite sample

4.e Ijolite

The concentrations of the REEs in the minerals of this rock are similar to that of the other silicate rocks from this complex. However, the low percentage of apatite and high percentage of diopside means that the majority of the HREE budget is stored in the diopside. If assumed that the perovskite is 1% of the rock when it was not reported in the rock (though it is in the sample we have) then it has between 60 and 30% of LREEs. The biotite that is a 14% percentage of this rock has no significant portion of the REE budget.

5. Discussion

5.a Mineral Comparisons

The largest advantage of analyzing these rocks by mineral is that there is an easy comparison between the different rock types. This also potentially allows for future comparison to different alkaline systems. This can be important for identifying what rocks have higher concentrations of REE than others. The primary minerals that is already used in this way are bastnaesite and monazite, the primary ore minerals for carbonatites. While there has been bastnaesite reported at the magnet cove complex, there was no evidence of it in these samples or in the Erikson and Blade mineralogical survey. However, in these samples there are both apatite and perovskite that seem the most appropriate for this comparison.

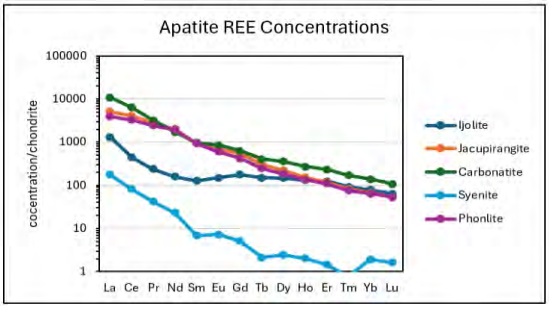

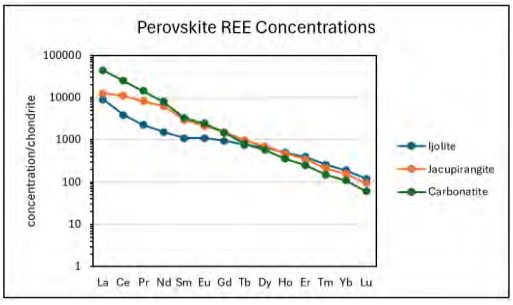

Figure 7a and 7b:a (on left) Compares the REE concentration of the apatite in each rock sample, 7b (right) Compares concentration of perovskite across the different samples it is present

With apatite appearing in all the rock types, it seems ideal for comparative analysis which was done in Ohly (2011). There is a great deal of similarity in the REE concentration between the rock types with the syenite and the ijolite deviating the most. The carbonatite apatite has a higher concentration of both LREEs and HREEs (figure 7a), while both the jacupirangite and the phonolite are about equal in concentrations. This could be an indication that there is a significantly higher concentration of REE seen in the rock.

The other mineral of interest that was analyzed was perovskite. In the carbonatite mineral approached the concentration of some ores (Benson and Watts 2024). However, in these rocks it did not incorporate a majority of the REE budget due to low abundance. If perovskites similar to these are seen in other rocks but with higher abundance those rocks could be an economic deposit.

5.b Whole rock comparisons

When comparing the whole rock concentrations of each of the rock types there is a very clear trend that emerges. The carbonatite has the highest LREE concentrations by about an order of magnitude over the silicate rocks. The HREE concentrations drop to about that of the silicates (fig. 8). When comparing that to the concentrations that are seen at Mountain Pass, Ca (fig. 9) there is similar trend. However, the concentrations for the Magnet Cove rocks are 100x lower than what is seen at Mountain Pass. This would mean that the source for these rocks was likely depleted in REEs before formation.

Figure 8 and 9: 8 (on left) Compares the REE concentration whole rock REE concentration at magnet cove with syenite being left off due to being below the start of the graph, 9 (right) Compares concentration of whole rock REE composition at mountain pass (Benson and Watts 2024)

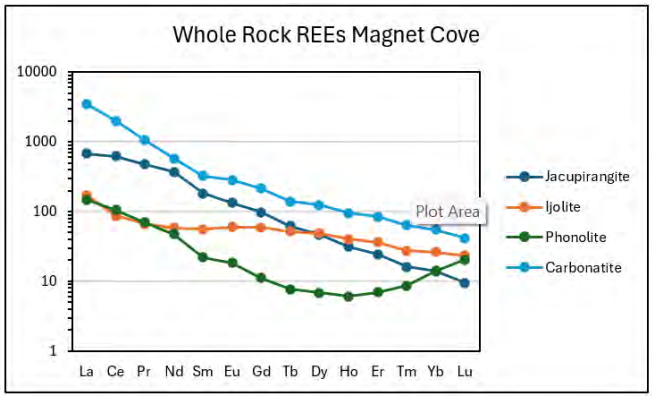

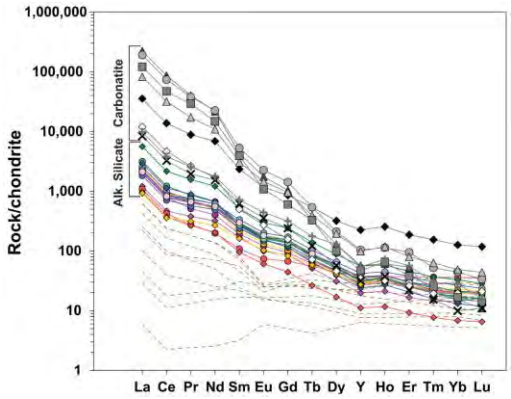

6.

CONCLUSION

Magnet cove when compared to Mountain Pass mine is depleted in REEs. The ore material from Mountain Pass has two order of magnitudes higher concentrations than that of the highest concentrations seen at Magnet Cove. The original source of Magnet Cove likely had low concentrations of REEs. This would seem to indicate that the first interpretation of the alternative hypothesis is the reason why Magnet Cove's carbonatite does not see high concentrations. While Magnet Cove is not a viable economic source of REEs it is valuable to know why some fail to form high concentration deposits.

BIBLIOGRAPHY

Anaenburg, M., Broom-Fendley,S., Chen, W., 2021, Formation of Rare earth Deposits in Carbonatites, Elements, v.17,327-332

Amaral, C., Lamb, A., Dumond G., 2024, Geophysical characterization of an alkaline-carbonatite complex using gravity and magnetic methods at Magnet Cove, Arkansas, USA, Tectonophysics, v. 893, 230545, ISSN 0040-1951, https://doi.org/10.1016/j.tecto.2024.230545.

Benson, E. and Watts, K., 2024, Apatite and Monazite Geochemistry Record Magmatic and Metasomatic Processes in Rare Earth Element Mineralization at Mountain Pass, California. *Economic Geology* 119 (7): 1611–1642. doi: https://doi.org/10.5382/econgeo.5108

Castor, S., 2008, Rare earth deposits of North America, Resource Geology, v.58, i.4, p.337-347, https://doi.org/10.1111/j.1751-3928.2008.00068.

Department of Energy, 2024, Developing a domestic supply of critical minerals and materials. Energy.gov. https://www.energy.gov/fecm/articles/developing-domestic-supply-critical-minerals-and-materials.

Erickson, R. and Blade, L.,1963, Geochemistry and Petrology of the Alkalic Igneous Complex at Magnet Cove, Arkansas, Geological Survey Professional Paper 425

Howard, M., and Chandler, A., 2007, Magnet Cove: a synopsis of its geology, lithology, and mineralogy, Arkansas geological survey.

McDonough, W., Sun, S., 1995, Chemical Geology, The composition of the Earth, v.120, p.223-253. https://doi.org/10.1016/0009-2541(94)00140-4.

Mitchell, R., 2005, Carbonatites and carbonatites and carbonatites. The Canadian Mineralogist, v. 43, p. 2049–2068. https://doi.org/10.2113/gscanmin.43.6.2049.

Ohly, R., 2011, Geochemistry of apatite from the carbonatite and associated alkaline rocks of the Magnet Cove Igneous Complex, Hot Spring County, Arkansas

Reich, M., Simon, A. C., 2024, Critical minerals, Annual Review of Earth and Planetary Sciences, v. 53, p. 13-40. https://doi.org/10.1146/annurev-earth-040523-023316.

Rowan, L., 2024, Critical Mineral Resources: National Policy and Critical Minerals List, Congressional Research Service, Report R47982.

Rudnick, R., Gao, S., 2003, Composition of the Continental Crust, Treatise in Geochemistry, v. 3, p. 1-64. https://doi.org/10.1016/B0-08-043751-6/03016-4.

Simandl, G., Paradis, S., 2018, Carbonatites: related ore deposits, resources, footprint, and exploration methods, Applied Earth Science, v. 127, p. 123-152, https://doi.org/10.1080/25726838.2018.1516935.

Wang, Z., Fan, H., Zhou, L., Yang, K., She, H., 2020, Carbonatite-Related REE Deposits: An Overview, Minerals, 10(11), 965, https://doi.org/10.3390/min10110965.

Winter, J. D., 2010, An introduction to igneous and Metamorphic Petrology. Pearson Education.

Yaxley, G. M., Anenburg, M., Tappe, S., Decree, S., & Guzmics, T., 2022, Carbonatites: Classification, sources, evolution, and emplacement, Annual Review of Earth and Planetary Sciences, v. 50, p. 261–293. https://doi.org/10.1146/annurev-earth-032320-104243.

Yang, J., Song, W., Liu, Y., Zhu, X., Kynicky, J., Chen, Q., 2024, Mineralogy and element geochemistry of the Bayan Obo (China) carbonatite dykes: Implications for REE mineralization, Ore Geology Reviews, Volume 165, 105873, ISSN 0169-1368, https://doi.org/10.1016/j.oregeorev.2024.105873.

Appendix 1

Photo 14

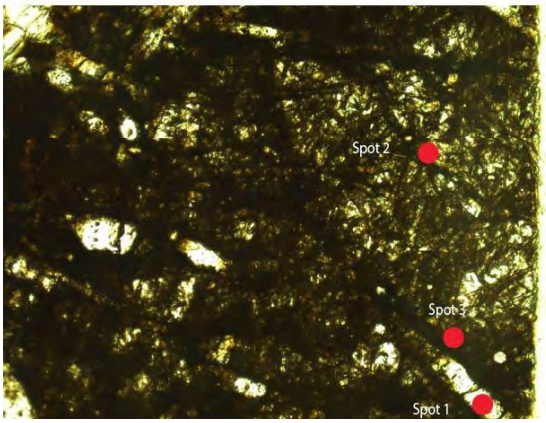

Spot 1 is apatite and spot 2 and 3 are montecellite

Photo 19

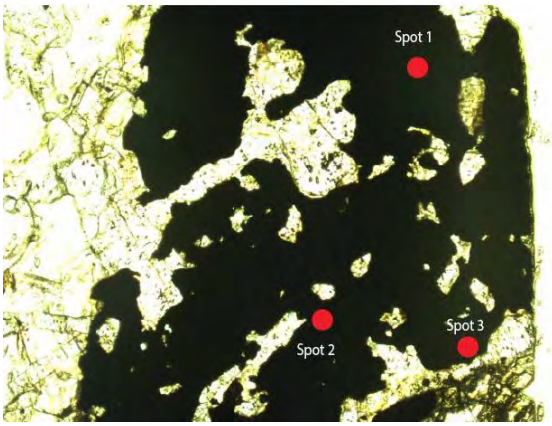

Opaque iron oxide surrounded by apatite

Photo 18

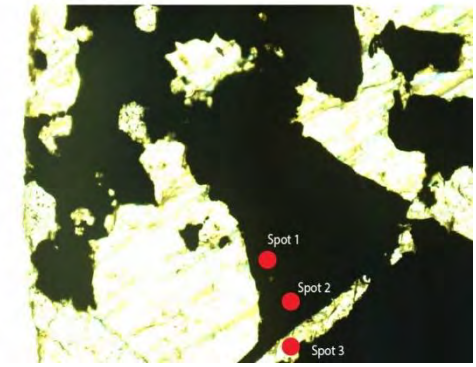

Iron oxide surrounded by calcite

Photo 10

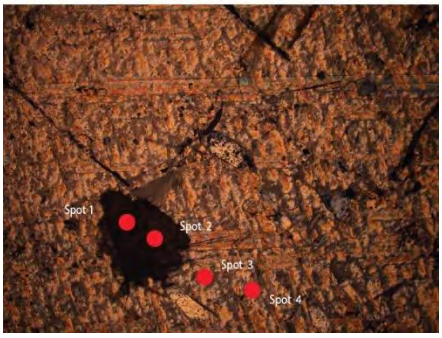

Perovskite surrounded by calcite

Photo 13

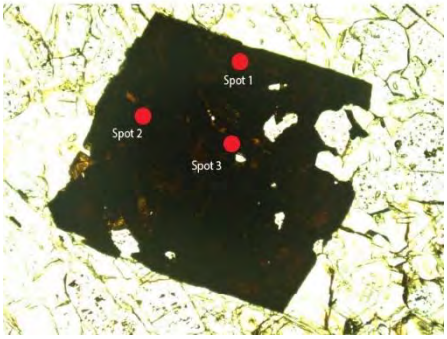

Perovskite surrounded by apatite

Photo 17

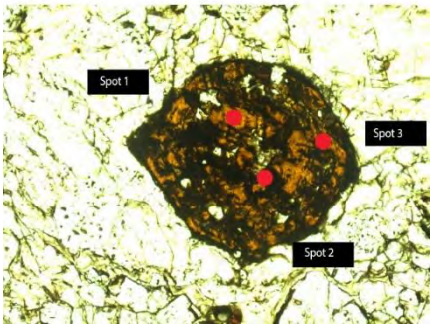

Kimzeyite surrounded by apatite

Photo 4

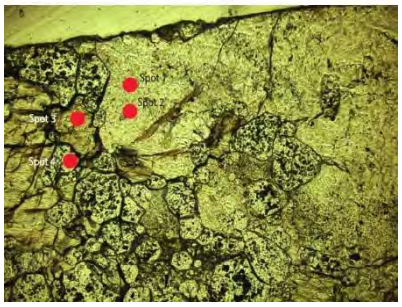

Apatite on left, calcite on right

Photo 11

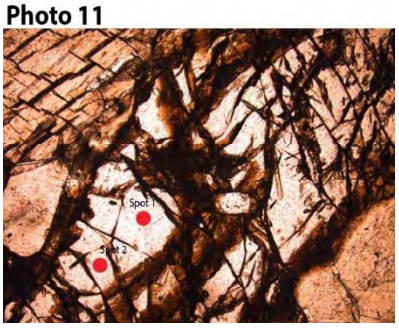

Montecellite

Appendix 2

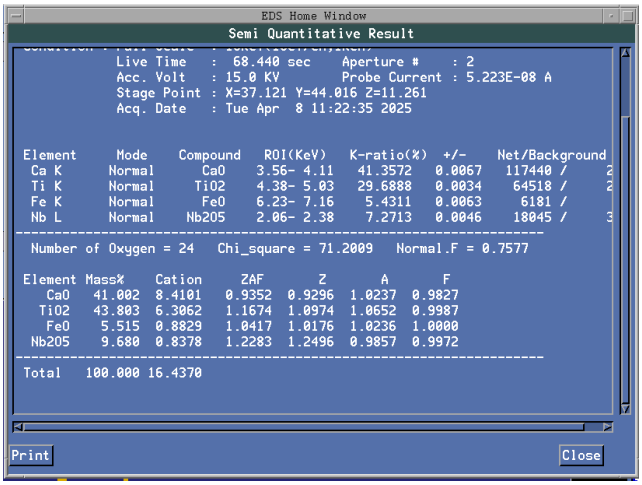

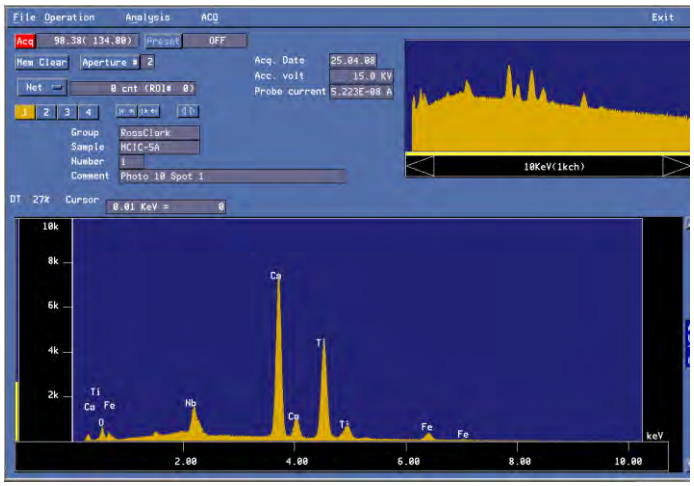

EDS 1: Perovskite

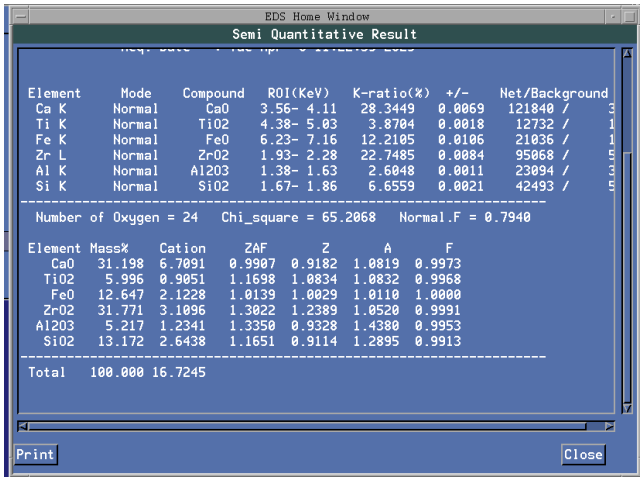

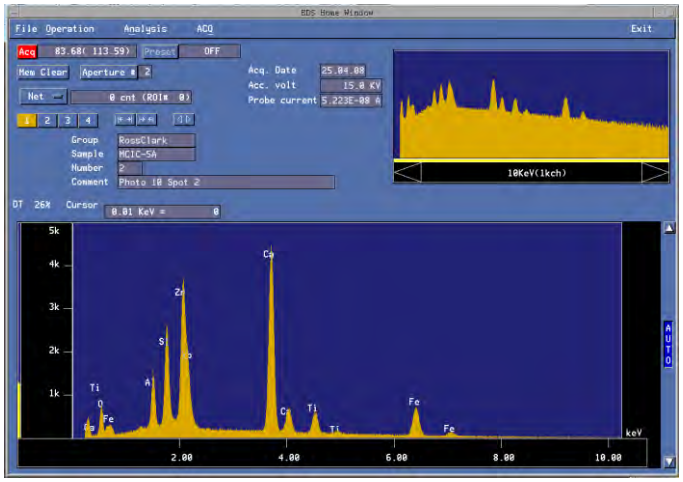

EDS 2: Kimzeyite

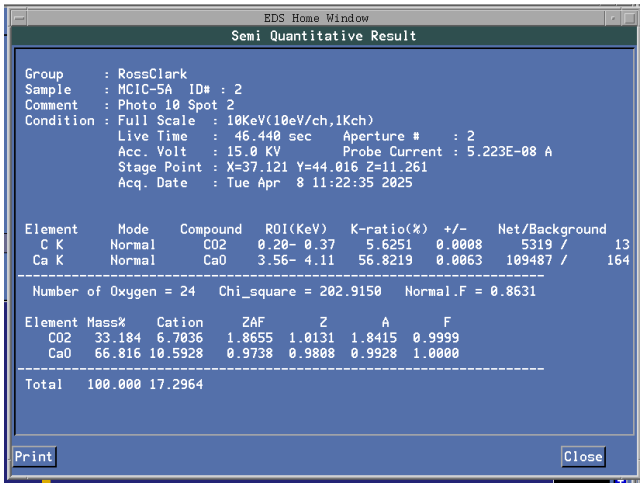

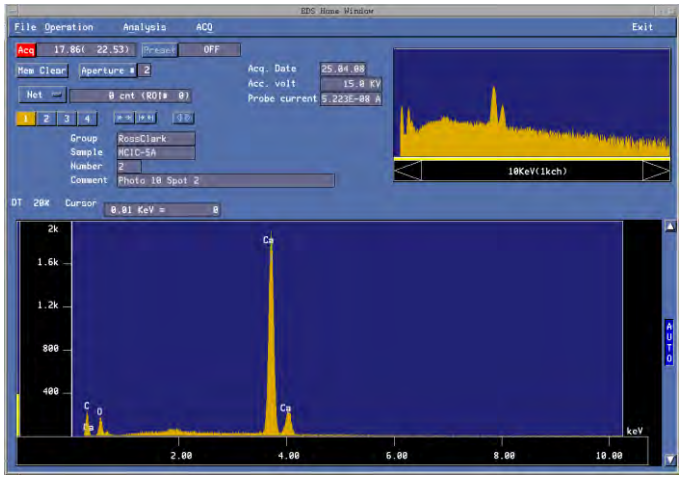

EDS 3: Calcite

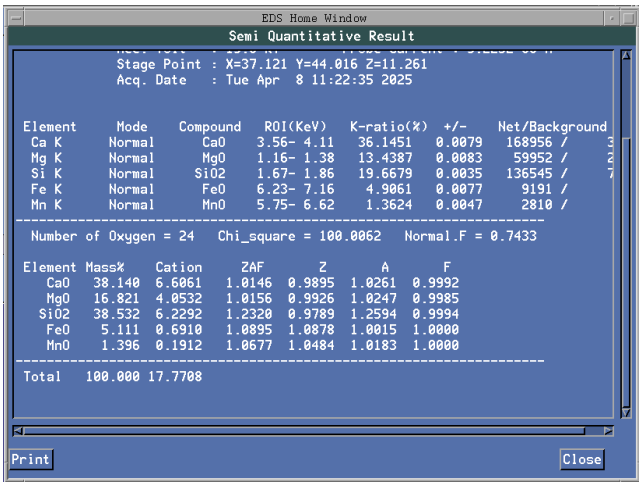

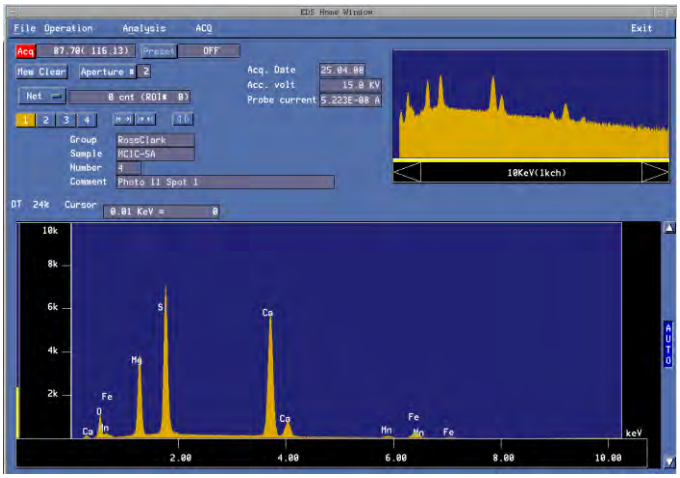

EDS 4: Montacellite

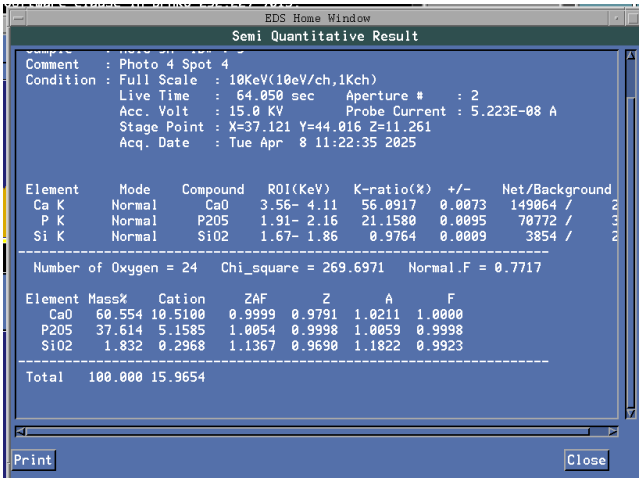

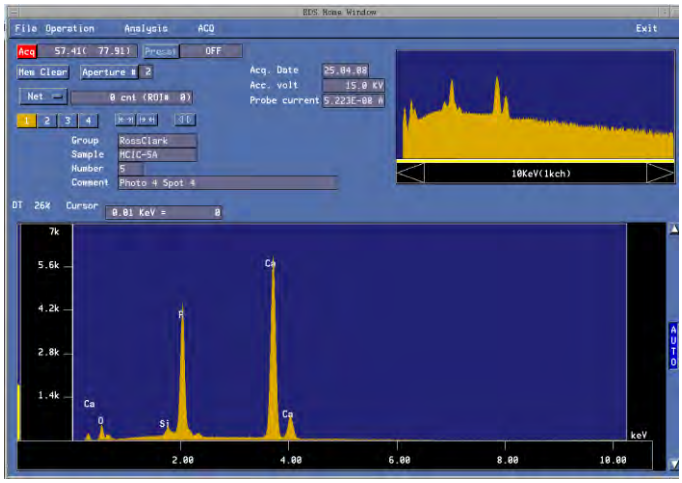

EDS 5: Apatite

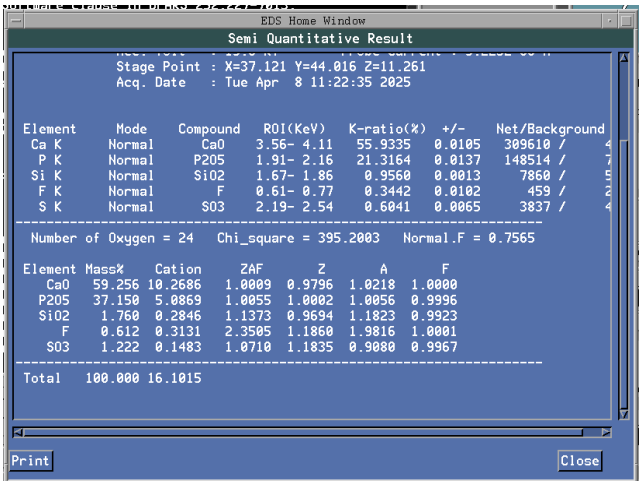

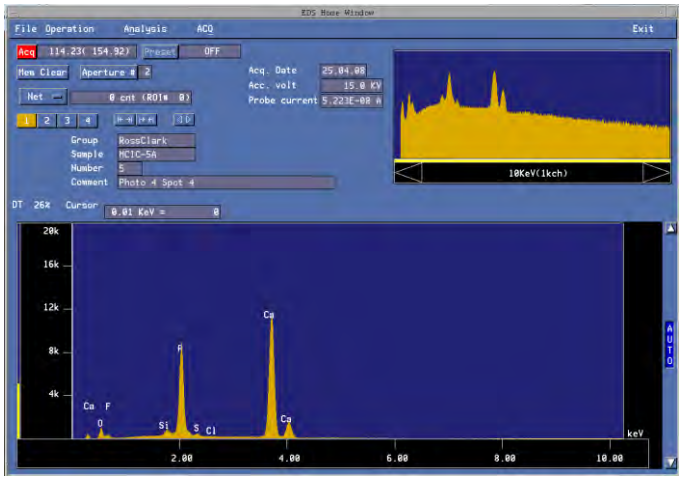

EDS 6: Fluoroapatite

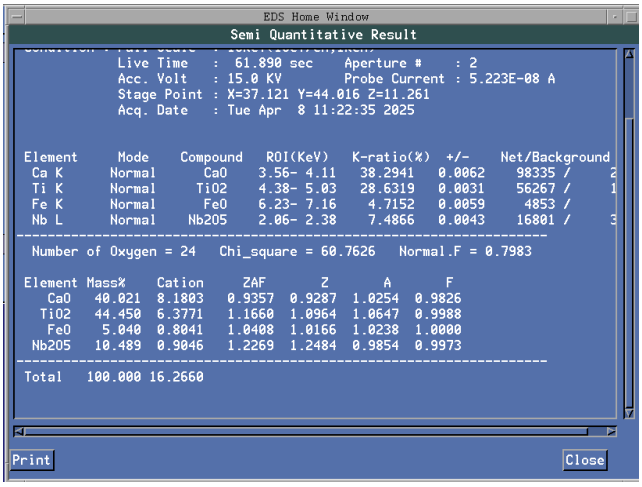

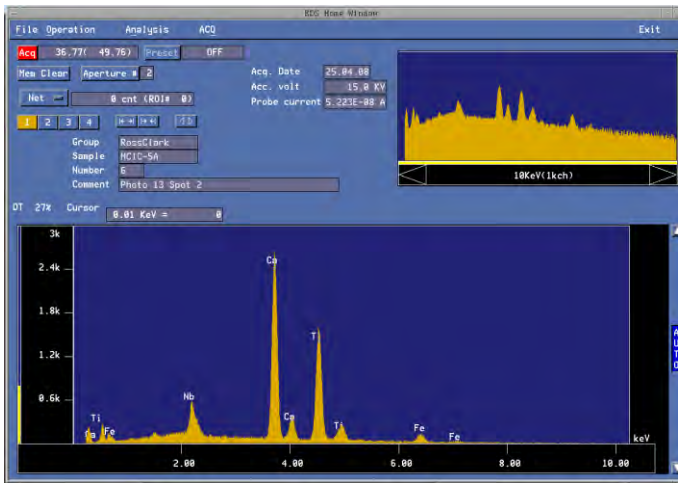

EDS7: Perovskite

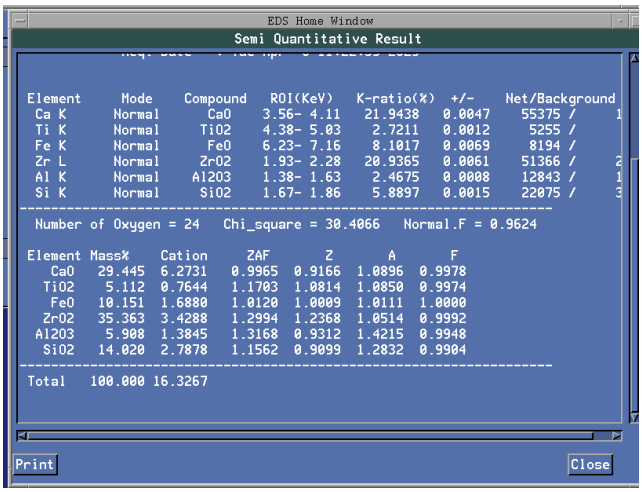

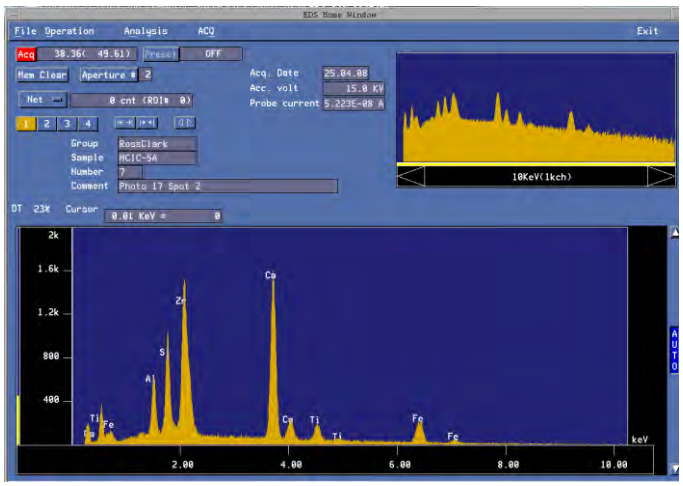

EDS 8: Kimzeyite

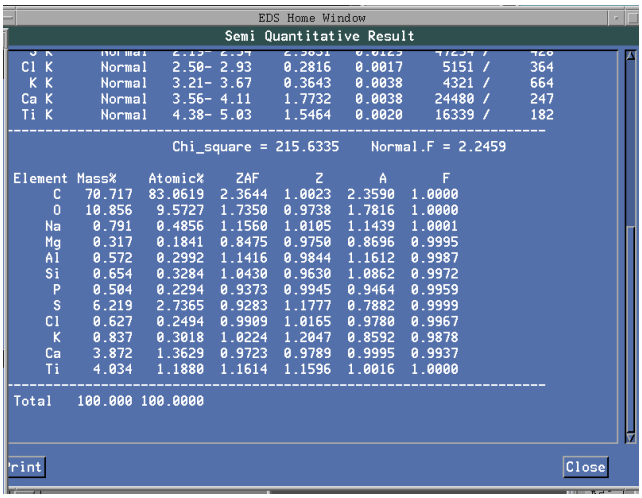

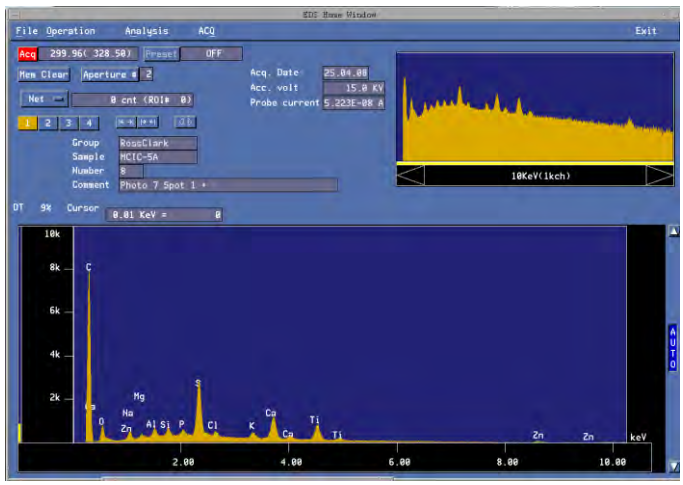

EDS 9: Growth on slide

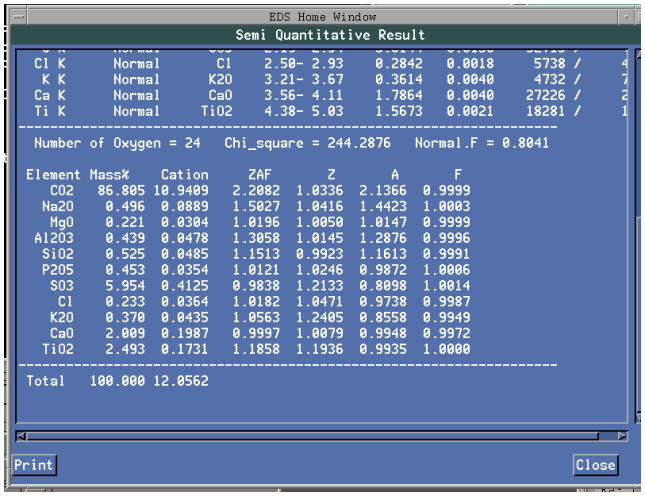

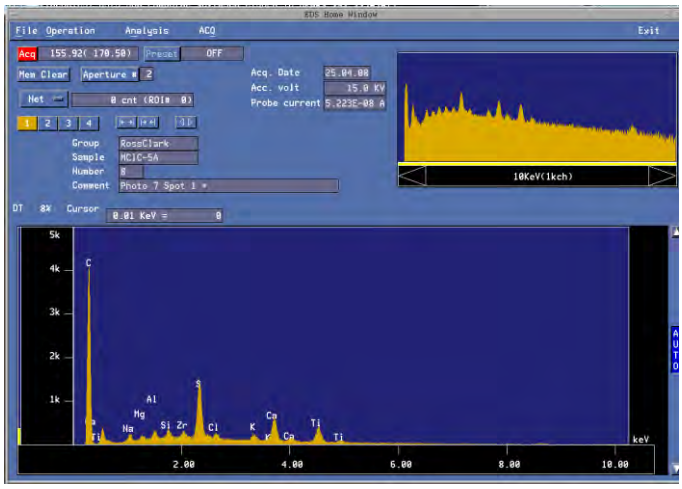

EDS 10: Growth on slide

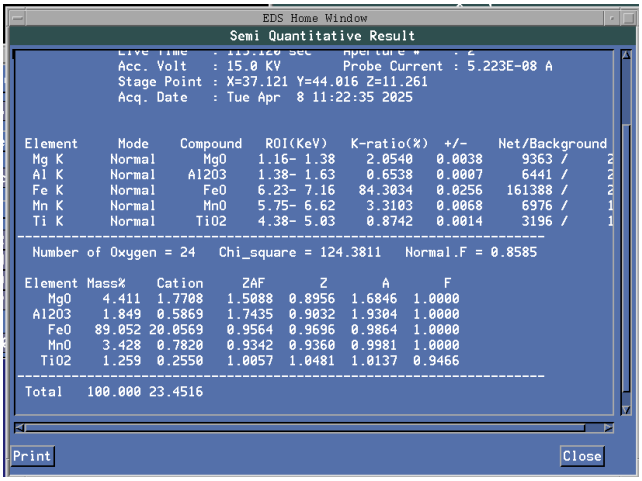

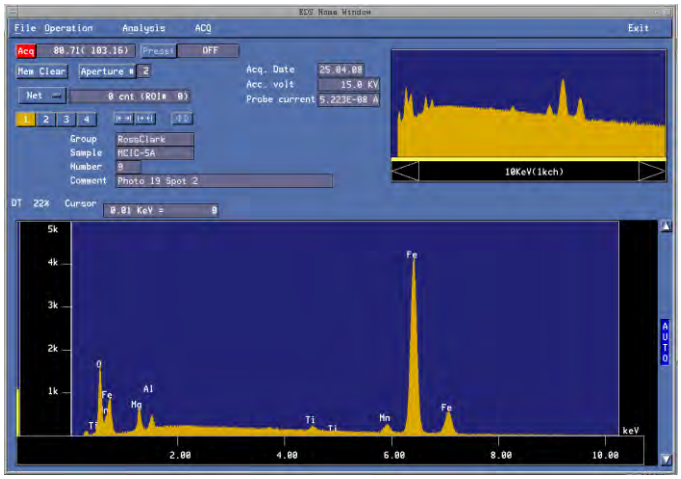

EDS 11: Magnetite/hematite

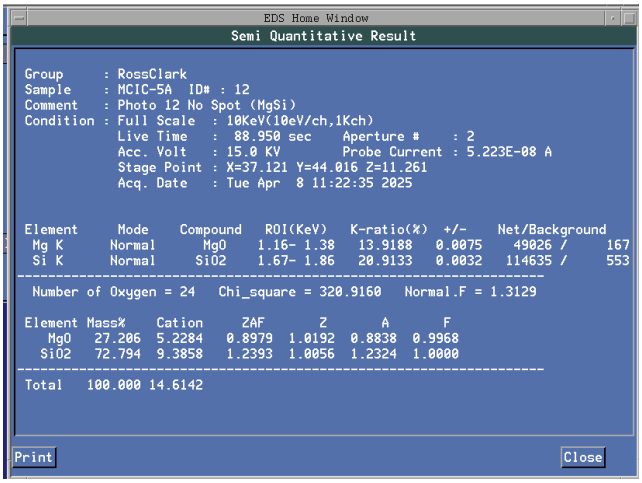

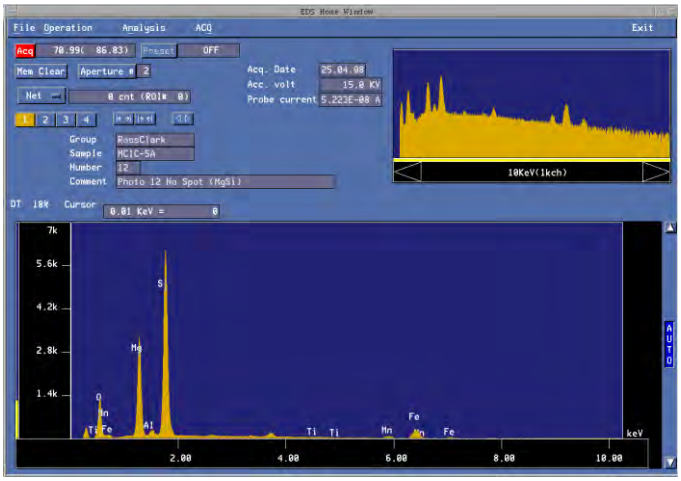

EDS 12:

Appendix 3

Trachyte-Phonolite

Pseudoleucite syenite

Biotite Ijolite

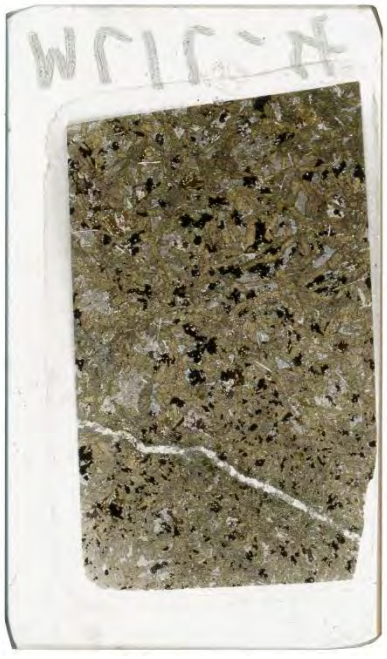

Jacupirangite

Carbonatite

Eds Data for MCIC 1-4

EDS	Sample	Photo	Label	SiO2	TiO2	Al2O3	FeO	MnO	MgO	CaO	Na2O	K2O	P2O5	SrO	F	CO2	Nb2O5	SO3	Fe	S	TOTAL
1	MCIC-1	Photo 1	EDS -1	63.17		21.25				3.8	3.86	7.97									100.05
2	MCIC-1	Photo 2	EDS-2	61.11		23.93				8.66	5.67	0.63									100
3	MCIC-1	Photo 2	EDS-3	36.17	6.19	13.55	24.6		7.48			11.26			0.74						99.99
4	MCIC-1	Photo 2	EDS-4		48.97		43.17	6									1.86				100
5	MCIC-1	Photo 2	EDS-5	43.76		3.08	24.21	2.91	2.31	23.73											100
8			EDS-8	34.71		3	25.96			36.34											100.01
9			EDS-9							54.68			45.32								100
11			EDS-11																44.4	55.59	99.99
12			EDS-12	41.21		22.92	27.76		6.44	1.66											99.99
13			EDS-13							63.18						36.81					99.99
14			EDS-14	1.9		0.877				53.04			44.18								99.997
16			EDS-16							70.41						29.59					100
17			EDS-17	40.67	3.63	14.01	7.69		22.19			11.8									99.99
18			EDS-18	45.53	54.01		0.46														100
19			EDS-19	44.38		34.31				17.91	3.4										100
20			EDS-20	25.44	17.55		20.9		1.2	34.9											99.99
21			EDS-21							65.28						34.72					100
22			EDS-22							54.31			45.69								100
23			EDS-23	41.16	15.57		5.45		24.46			13.37									100.01
24			EDS-24	44.71		34.59				17.59	3.11										100
25			EDS-25	32.63	3.89	2.83	23.586			37.07											100.01
26			EDS-26	56.61		30.18					13.21										100
27			EDS-27	33.29	5.13	2.17	21.94			37.47											100
28			EDS-28							55.54			44.46								100
29			EDS-29							54.86			45.14								100
30			EDS-30	53.63		31.96				4.38	10.06										100.03
31			EDS-31	43.49	3.52	5.96	10.55		10.02	26.46											100
32			EDS-32		2.83		97.17														100
33			EDS-33		51.6		40.16	8.24													100
34			EDS-34	28.701	39.19	0.829				31.28											100
35			EDS-35	36.99	3.28	14.86	17.84		14.79			12.24									100
36			EDS-36	45.16	3.75	5.32	10.81		9.8	25.15											99.99
37			EDS-37		57.91					42.09											100
38			EDS-38	28.62	39.16	1.03				31.18											99.99
39			EDS-39	40.04		30.69				9.74	13.59							5.94			100
40			EDS-40	43.34	3.23	6.3	11.44		9.89	25.79											99.99
41			EDS-41		8.68		91.31														99.99
42			EDS-42	63.41																	63.41
43			EDS-43	55.17		25.99					18.84										100
44			EDS-44				100														100
45			EDS-45	64.25		17.2					0.29	18.26									100
46			EDS-46																42.38	57.62	100
47			EDS-47	63.67		16.89					0.29	19.15									100
48			EDS-48	57.53		33.21				3.09	6.19										100.02
49			EDS-49							52.96			47.04								100
50			EDS-50				100														100
51			EDS-51					6.91		93.09											100
52			EDS-52							64.26			35.76								100.02

Appendix 4

All concentration data collected from LA-ICP-MS

140Ce	141Pr	142Nd	144Nd	146Nd	147Sm	151Eu	152Sm	153Eu	154Sm	155Gd	157Gd	159Tb	161Dy	163Dy	165Ho	166Er	169Tm	172Yb	175Lu	178Hf	181Ta	182W	232Th	238U
455	469	451	453	451	482	478	492	480	483	475	480	473	470	470	482	489	472	488	481	474	487	483	497	495
444	467	434	444	443	465	473	468	468	461	462	459	455	450	450	478	473	457	466	459	447	462	447	478	473
32	4.7	25	22	24	6.1	2.1	6.4	2.0	6.1	6.4	6.3	0.800	5.2	5.1	0.893	2.4	0.30	2.0	0.24	4.2	1.1	0.17	1.1	0.33
33	4.8	26	22	24	6.0	2.1	6.1	2.1	6.1	6.4	6.0	0.770	5.0	4.9	0.900	2.5	0.29	1.8	0.26	4.2	1.0	0.21	1.1	0.36
4272	323	1959	842	948	149	52	144	52	143	254	139	16	96	95	16	41	4.6	25	2.9	0.053	0.026	2.7	0.51	36
2238	196	1066	500	534	83	29	83	30	82	148	79	9.3	56	55	9.3	23	2.6	15	1.8	0.024	0.009	0.033	0.91	20
1326	110	777	320	369	76	27	76	26	77	138	100	17	135	137	31	110	18	128	20	0.087	0.012	14	0.57	20
0.653	0.059	0.320	0.164	0.182	0.025	0.008	0.026	0.008	0.024	0.045	0.019	0.002	0.012	0.011	0.002	0.004	0.000	0.002	0.000	0.000	0.000	0.007	0.000	0.010
0.168	0.007	0.039	0.023	0.024	0.004	0.004	0.004	0.001	0.004	0.007	0.004	0.000	0.002	0.003	0.000	0.001	0.000	0.001	0.000	0.001	0.000	0.001	0.000	0.001
2877	233	1359	648	690	108	38	109	37	108	182	103	11	67	67	11	27	2.9	16	1.8	0.026	0.009	0.076	0.32	13
0.029	0.000	-0.003	-0.001	-0.001	-0.002	-0.001	-0.001	0.000	-0.002	0.000	0.000	0.000	0.001	0.000	0.000	0.000	0.000	0.001	0.000	0.018	0.000	0.000	0.000	0.000
0.001	0.000	0.000	0.000	0.000	0.000	0.000	-0.001	0.000	0.000	0.000	0.000	0.000	0.000	0.000	0.000	0.000	0.000	0.000	0.000	0.003	0.000	0.000	0.000	0.000
3399	274	1622	723	798	123	43	123	44	122	217	118	14	83	82	14	35	3.9	20	2.4	0.13	0.007	0.056	0.34	18
446	455	431	436	430	458	454	460	456	460	450	451	447	445	448	461	458	442	457	444	440	458	425	462	448
397	411	394	390	393	421	410	421	420	421	415	416	410	404	409	421	424	406	420	415	408	425	407	435	428
32	4.8	25	22	24	6.2	2.1	6.1	2.1	6.2	6.3	5.9	0.80	5.1	5.2	0.868	2.4	0.29	1.993	0.25	4.1	1.1	0.27	1.1	0.33
33	4.6	27	21	30	5.8	2.0	6.0	2.0	5.9	5.9	5.8	0.78	4.7	4.8	0.868	2.3	0.29	1.904	0.25	4.2	1.1	0.23	1.1	0.33
16096	1379	7764	3781	4201	501	140	518	143	490	876	305	30	150	147	20	42	4.0	19	1.6	22	42	10	2.0	143
666	93	531	441	473	164	68	162	68	163	199	191	32	231	230	43	120	16	105	11	653	6.4	0.10	0.15	112
29	3.0	25	6.0	6.7	1.1	0.46	0.99	0.46	1.1	3.1	2.8	0.14	0.80	0.85	0.16	0.49	0.062	0.42	0.058	0.021	0.000	0.000	0.039	0.23
30	2.2	13	6.1	7.3	0.96	0.35	0.94	0.41	0.99	3.1	2.0	0.13	0.80	0.79	0.15	0.44	0.056	0.36	0.052	0.000	0.003	-0.001	1.4	0.93
15545	1346	7553	3701	4065	479	136	515	138	487	843	297	29	144	141	19	40	3.6	17	1.4	18	45	7.450	2.0	132
14453	1244	7024	3443	3751	460	129	482	130	451	797	282	28	139	135	18	39	3.6	17	1.4	23	40	9.033	2.1	131
0.107	0.009	0.050	0.024	0.026	0.003	0.001	0.003	0.001	0.003	0.006	0.003	0.000	0.002	0.002	0.000	0.001	0.000	0.000	0.000	0.000	0.000	0.000	0.000	0.001
536	79	460	412	419	149	61	147	62	149	181	176	29	207	206	38	103	13	85	8.4	733	9.9	0.087	0.16	88
612	86	502	407	430	150	63	150	64	152	185	181	30	213	212	39	107	14	86	8.6	719	10	0.11	0.096	91
572	78	451	385	409	145	61	145	61	146	178	173	29	206	205	38	104	14	84	8.4	694	8.9	0.13	0.12	93
462	446	442	430	429	447	435	441	439	446	444	445	425	427	423	436	446	424	443	430	432	435	453	452	458
436	435	437	424	424	440	436	437	429	436	441	436	417	417	419	430	440	418	429	416	415	421	420	438	444
35	4.8	27	21	23	6.2	2.1	5.8	2.1	5.9	6.6	5.7	0.79	4.839	5.0	0.83	2.3	0.28	1.9	0.25	3.9	1.0	0.16	1.1	0.32
32	4.6	28	24	23	6.2	2.0	5.9	2.8	5.9	5.9	5.9	0.75	4.974	4.8	0.87	2.3	0.38	1.8	0.26	4.1	1.1	0.18	1.1	0.34
23	1.8	11	4.3	4.8	0.72	0.46	0.74	0.39	0.90	2.5	3.0	0.078	0.43	0.52	0.10	0.32	0.041	0.25	0.035	0.002	0.000	0.004	0.000	0.000
23	1.7	10	4.6	5.1	0.78	0.29	0.74	0.29	0.81	2.6	2.0	0.10	0.58	0.55	0.10	0.31	0.042	0.30	0.038	0.003	0.000	0.001	0.011	0.000
22	2.6	9.9	5.0	4.9	0.74	0.27	0.80	0.32	0.79	2.5	2.0	0.092	0.62	0.61	0.11	0.34	0.044	0.28	0.039	-0.002	0.000	0.008	0.003	0.001
3983	304	1818	790	883	132	46	131	48	129	230	124	14	84	84	14	36	4.1	22	2.6	0.067	0.007	0.25	0.36	36
21	2.6	17	10	8.1	3.4	1.6	3.5	1.7	3.8	6.5	6.4	1.3	12	12	2.9	11	1.7	13	2.1	0.016	0.012	0.003	0.022	0.025
66	3.3	22	9.7	13	3.7	1.8	3.9	1.8	4.0	6.6	6.7	1.4	11	11	2.7	9.4	1.5	11	1.7	0.004	0.005	0.000	0.009	0.036
103	8.4	49	23	25	3.9	1.3	3.8	1.4	3.8	6.8	3.6	0.42	2.6	2.5	0.42	1.1	0.12	0.65	0.079	0.004	0.003	0.003	0.010	0.88
533	445	423	428	427	444	435	445	434	449	438	443	424	434	428	430	446	422	436	420	420	429	436	428	456
468	464	435	445	452	476	462	467	454	476	475	469	449	456	455	457	469	444	467	451	449	454	492	471	500
33	5.0	27	21	23	5.8	2.0	5.9	2.0	5.9	6.1	5.9	0.81	4.9	4.8	0.87	2.3	0.30	1.8	0.22	4.0	1.1	0.18	0.97	0.31
35	4.4	26	23	22	5.6	1.8	5.4	1.9	5.3	5.8	5.4	0.73	4.5	4.6	0.83	2.1	0.27	1.6	0.23	3.8	0.97	0.19	1.1	0.31
0.046	0.111	0.073	0.222	0.062	0.015	0.002	0.011	0.001	0.005	0.015	0.001	0.003	0.024	0.018	0.004	0.009	0.001	0.020	0.002	0.029	0.30	0.065	0.003	0.037

			7Li	23Na	25Mg	26Mg	27Al	29Si	30Si	31P	43Ca	45Sc	47Ti	49Ti	51V	55Mn	57Fe	59Co	60Ni	61Ni	63Cu	64Zn	66Zn	86Sr	88Sr	89Y	90Zr	91Zr	93Nb	97Mo	98Mo	133Cs	137Ba	138Ba	139La	1
2	NIST		468	13	417	396	2.00	33	32	255	8.21	465	434	433	442	463	0	410	456	467	428	455	457	520	530	481	459	465	483	417	431	377	471	478	465	
3	NIST		479	14	418	400	2.02	33	34	258	8.21	457	435	439	459	437	0	414	444	469	454	469	440	501	526	482	468	461	478	401	406	373	466	475	462	
4	BHVO		3.7	1.9	43554	41018	16	24	23	657	8.14	31	18683	19144	280	1238	5.8	37	104	109	105	94	95	407	418	20	157	157	16	3.4	3.9	0.072	139	131	14	
5	BHVO		4.0	2.0	44804	40786	15	24	24	651	8.14	30	18834	19628	281	1285	6.0	39	109	122	110	99	96	419	429	20	158	155	16	3.5	3.2	0.149	141	131	14	
6	photo 14		0.260	0.091	106	163	0.025	0.572	0.75	88670	39	0.44	230	13	616	51	0.021	11	2.0	24	7.5	3.0	2.7	3705	3338	477	41	42	1.7	0.93	9.2	17	701	1050	2766	
7	spot 18		5.8	0.054	13416	12328	0.118	1.6	1.8	60373	27	0.54	100	2.4	416	842	0.28	8.4	2.3	18	1.1	13	22	2368	2125	289	22	23	0.20	0.094	0.19	0.50	97	110	1625	
8	spot 19		1428	0.417	791022	743550	0.660	114	112	38499	27	36	572	365	311	71828	23	336	5.9	45	55	863	861	7565	7193	990	38	35	2.9	1.7	2.4	10	756	711	1729	
9	Photo19		0.001	0.000	3.280	2.979	0.000	0.000	0.000	1.437	0.001	0.001	4.588	4.713	0.039	1.522	0.003	0.007	0.000	0.001	0.001	0.081	0.080	0.160	0.159	0.039	0.041	0.038	0.027	0.000	0.000	0.000	0.018	0.020	0.505	
10	spot 20		0.047	0.000	175	164	0.021	0.001	0.002	2.100	0.001	0.111	41	37.055	2.105	114.356	0.217	0.537	0.012	0.018	0.001	5.340	5.453	0.163	0.158	0.011	0.064	0.063	0.001	0.001	0.000	0.000	0.372	0.345	0.069	
11	spot 21		5.2	0.054	5176	5510	0.410	0.53	0.86	91158	39	0.73	332	60	604	825	1.1	22	1.9	24	2.7	33	35	3235	2980	336	11	12	0.422	0.475	0.873	1.269	410	447	1888	
12	Photo18		0.558	0.000	2103	1913	0.419	0.002	0.003	-0.038	0.001	0.927	537	541	11	772	1.523	3.8	0.046	0.083	0.005	33.312	33.702	0.218	0.048	0.000	1.144	1.125	0.063	0.006	0.002	0.022	-0.019	-0.001	0.001	
13	spot 24		0.100	0.000	345	318	0.065	0.000	0.003	0.008	0.001	0.163	91	94.886	1.694	133	0.265	0.657	0.007	-0.002	0.004	5.750	5.797	0.997	0.940	0.000	0.152	0.152	0.008	0.001	0.000	0.000	0.001	0.002	0.001	
14	spot 25		0.72	0.053	293	203	0.053	0.38	0.41	88293	39	0.68	227	29	546	105	0.134	18	1.5	20	1.2	6.5	3.5	3189	2940	430	26	26	0.085	0.086	0.036	0.053	10	20	2317	
15	NIST		465	14	436	457	2.0	33	33	583	8.21	459	446	441	444	451	0	402	464	433	437	461	454	510	527	478	459	459	470	419	405	365	449	453	443	
16	NIST		422	12	392	411	1.8	30	30	293	8.21	425	390	392	412	397	0	369	399	414	391	402	397	467	476	433	423	414	424	371	368	324	415	405	400	
17	BHVO		3.8	1.9	43866	41002	15	24	23	658	8.14	31	18671	19595	280	1266	5.9	38	107	106	109	96	95	403	423	20	158	159	16	4.0	3.8	0.087	141	133	17	
18	BHVO		3.9	1.9	43350	40150	15	23	23	662	8.14	29	18519	18908	283	1260	5.8	39	109	114	107	95	94	403	409	19	153	150	16	4.3	6.7	0.41	135	127	13	
19	Photo 10		0.29	0.210	390	324	0.770	0.054	0.125	711	29	6.8	243452	249754	176	137	2.5	0.44	0.23	8.6	3.6	25	6.9	2039	1870	379	4790	4800	57057	0.35	0.53	0.043	3.8	72	11159	
20	Spot 27		0.72	0.034	2272	2095	7.2	4.5	4.9	4.4	22	673	35049	35208	35	513	5.9	1.3	0.17	8.6	0.40	24	20	94	86	1112	231503	233115	4989	0.051	0.010	0.037	0.099	3.5	251	
21	Spot 28		0.000	0.001	227	218	0.000	0.050	-0.006	-2.517	40	0.036	-0.309	0.070	0.010	62	0.024	0.10	0.25	17	0.33	1.4	0.19	5683	5256	5.9	0.37	0.067	-0.005	0.28	0.003	-0.001	99	98	37	
22	Spot 29		0.032	0.002	231	212	0.000	-0.005	0.048	-0.160	40	0.041	16	0.99	0.004	64	0.019	0.26	1.2	14	0.24	0.82	0.30	5584	5152	5.8	0.70	1.8	0.027	0.06	0.092	0.002	68	70	40	
23	Photo 13		0.20	0.22	305	266	0.77	0.043	-0.039	39	29	6.0	240753	246777	157	130	2.3	0.46	0.26	8.2	2.7	26	4.0	1841	1657	374	4001	4014	51745	0.41	0.23	0.041	3.6	68	10661	
24	Spot 31		0.16	0.13	304	262	0.73	0.041	0.147	1.6	29	6.7	238226	245533	162	126	2.3	0.41	0.20	9.8	2.6	26	3.9	1907	1748	365	4751	4787	52324	0.48	0.333	0.055	2.5	62	9853	
25	Spot 32		0.000	0.000	0.007	0.004	0.000	0.000	0.000	1.314	0.001	0.000	0.667	0.668	0.010	0.002	0.000	0.000	0.000	0.000	0.000	0.000	0.000	0.094	0.083	0.008	0.015	0.013	0.130	0.000	0.000	0.000	0.001	0.001	0.071	
26	Photo 17		0.567	0.039	1533	1438	7.3	3.9	4.3	0.349	21.1	473	31094	31432	23	465	5.3	1.3	0.18	8.164	-0.388	24	22	98	84	961	228680	230260	5671	0.17	0.020	0.006	5.2	7.0	187	
27	Spot 34		4.2	0.046	1637	1507	7.5	4.1	4.3	1263	21.1	468	31658	31989	33	543	5.3	1.4	0.16	11	0.39	23	22	215	220	999	228967	226652	5645	0.20	0.047	0.008	157	162	239	
28	Spot 35		0.838	0.152	1594	1474	7.2	3.9	4.3	21	21.1	483	30081	30629	24	449	5.2	1.5	0.13	11	0.39	23	22	243	251	948	223770	223704	5667	0.41	0.210	0.012	28	28	177	
29	NIST		474	14	502	388	2.0	35	33	506	8.21	465	514	510	451	465	0.06	426	473	482	457	467	468	536	520	454	440	450	462	442	419	376	443	446	443	
30	NIST		453	13	410	549	1.9	32	32	414	8.21	441	470	501	425	420	0.04	394	465	442	428	454	463	487	493	445	430	431	457	412	415	352	459	438	423	
31	BHVO		4.0	2.1	44242	41328	15	24	24	746	8.14	32	18913	19413	287	1315	6.169	40	111	113	115	107	101	412	419	20	156	158	20	3.5	7.0	0.14	140	131	15	
32	BHVO		6.0	2.0	44051	40190	15	24	23	835	8.14	31	18757	19294	285	1286	5.989	53	111	115	114	96	96	404	412	20	156	154	16	3.7	3.2	0.086	138	129	13	
33	Photo 4		0.002	0.002	216	162	0.000	0.085	0.037	0.381	40	0.058	-0.185	-0.455	0.031	78	0.028	0.10	0.43	15	0.190	-0.116	0.33	5918	5237	3.8	-0.025	-0.116	0.011	0.14	-0.009	-0.007	136	124	30	
34	Spot 37		0.032	0.001	254	181	0.000	0.019	0.088	1.428	40	0.019	8.9	0.072	-0.005	86	0.019	0.11	0.57	16	1.1	2.5	0.83	6132	5260	4.1	-0.022	0.308	0.004	0.23	0.007	0.42	70	70	31	
35	Spot 38		0.004	0.001	176	162	0.000	0.068	0.037	1.317	40	0.033	0.008	0.23	0.011	81	0.019	0.11	0.40	13	0.129	1.0	0.18	5527	5190	4.4	0.088	0.023	1.7	0.84	0.010	0.010	77	74	32	
36	Spot 39		0.089	0.074	499	379	0.006	0.608	0.862	90047	40	0.502	189	1.1	635	69	0.030	13	1.5	21	0.905	1.1	1.1	3418	3065	459	53	54	0.84	0.076	0.095	1.1	7.6	25	2640	
37	Photo 11		4.3	0.012	137704	132383	0.004	16	15	72	27	4.5	44	41	1.6	8965	2.9	35	0.44	11	0.326	84	85	66	57	93	1.3	1.4	0.41	0.082	0.089	0.056	0.77	0.49	9.8	
38	Spot 41		0.79	0.010	139053	129424	0.002	14	14	440	27	4.2	52	38	0.85	8760	2.9	31	0.54	8.4	0.065	79	82	59	55	85	1.7	1.3	3.2	5.1	-0.016	0.857	0.004	0.31	11	
39	Photo 7		0.002	0.003	22.120	18	0.002	0.016	0.020	2687	1.4	0.016	30	30	19	3.389	0.001	0.34	0.33	0.89	2.1	17	18	125	114	13	1.1	1.1	0.15	0.011	0.005	0.001	0.62	0.92	74	
40	NIST		508	13	442	440	1.9	32	34	734	8.21	459	449	450	485	454	0.05	428	483	494	446	483	492	521	526	451	444	446	469	434	440	375	450	455	436	
41	NIST		488	14	450	414	2.0	35	35	291	8.21	476	495	461	496	479	0.04	451	503	484	504	506	529	600	538	480	468	466	487	455	468	398	469	477	457	
42	BHVO		3.8	1.9	42645	39601	15	23	23	686	8.14	31	18853	19383	288	1224	5.7	40	105	113	106	96	91	425	408	20	157	154	16	5.2	3.1	-1.080	136	129	14	
43	BHVO		3.6	2.0	41142	38216	14	22	22	955	8.14	30	17907	18629	271	1211	5.5	37	107	107	103	89	91	381	395	19	153	147	15	3.8	3.3	0.085	128	119	14	
44	Photo 20	bizarre	0.026	0.016	159	151	0.010	0.010	0.002	272	1.4	0.015	2658	2617	0.182	1.9	0.005	0.015	0.75	1.4	8.1	1274	1334	9.5	8.4	0.23	1.2	1.2	8.1	0.024	0.030	0.028	2.5	1.9	0.080	